EARTHQUAKE ENGINEERING AND STRUCTURAL DYNAMICS
Earthquake Engng Struct. Dyn. 2000; **29**: 629–645

Forced vibration test of a building with semi-active damper system

Narito Kurata[1,*], Takuji Kobori[1,†], Motoichi Takahashi[1], Toshihisa Ishibashi[2], Naoki Niwa[1], Jun Tagami[2] and Hiroshi Midorikawa[2]

[1]*Kobori Research Complex, Kajima Corporation, KI Building, 6-5-30, Akasaka, Minato-ku, Tokyo 107-8502, Japan*
[2]*Kajima Technical Research Institute, 2-19-1, Tobitakyu, Chofu-shi, Tokyo 182-0036, Japan*

SUMMARY

The authors developed a semi-active hydraulic damper (SHD) and installed it in an actual building in 1998. This was the first application of a semi-active structural control system that can control a building's response in a large earthquake by continuously changing the device's damping coefficient. A forced vibration test was carried out by an exciter with a maximum force of 100 kN to investigate the building's vibration characteristics and to determine the system's performance. As a result, the primary resonance frequency and the damping ratio of a building that the SHDs were not jointed to, decreased as the exciting force increased due to the influence of non-linear members such as PC curtain walls. The equivalent damping ratio was estimated by approximating the resonance curves using the steady-state response of the SDOF bilinear hysteretic system. After the eight SHDs were jointed to the building, the system's performance was identified by a response control test for steady-state vibration. The elements that composed the semi-active damper system demonstrated the specified performance and the whole system operated well. Copyright © 2000 John Wiley & Sons, Ltd.

KEY WORDS: structural control; semi-active control; semi-active hydraulic damper; forced vibration test; linear quadratic regulator; velocity feedback

1. INTRODUCTION

A lot of research and development has been carried out on semi-active devices and control strategies during the past several years because of their high-performance and small-energy requirement [1, 2]. To promote development and application of on–off semi-active hydraulic dampers that can switch an internal valve to fully open or fully close, Kobori *et al.* [3] installed a system in an actual three-storey building and Patten *et al.* [4] attached it to an in-service bridge. However, the authors proposed the application of a semi-active structural control system

* Correspondence to: Narito Kurata, Kobori Research Complex, Kajima Corporation, KI Building, 6-5-30, Akasaka, Minato-ku, Tokyo 107-8502, Japan
† Professor Emeritus of Kyoto University, Dr of Eng., Chief Executive Adviser, Kajima Corporation

Received 6 August 1999
Revised 8 October 1999
Accepted 20 October 1999

utilizing fully continuously variable damping elements to a building structure in 1991 [5]. Kurata *et al.* demonstrated the effectiveness of this system through a control experiment on a large three-storey model structure using a shaking table [6] and a simulation analysis of a semi-actively controlled building in large earthquakes [7, 8]. In 1998, the authors developed a continuously variable semi-active hydraulic damper (SHD) with a maximum damping force of 1000 kN with an electric power of 70 W, and installed it in an actual building. This was the first application of a semi-active structural control system that can control the response of a building in a large earthquake by continuously changing the valve opening rate (equivalent to damping coefficient) of the damper. Kurata *et al.* [9] reported the details of the building, the control system configuration, the SHD, a control method by a linear quadratic regulator (LQR), the response analysis results for the controlled building, and the dynamic loading test results of the actual SHD. This semi-active damper system is designed to control the building's response in linear range during a large earthquake.

This paper presents the results of a forced vibration test on the building by an exciter with a maximum force of 100 kN. The characteristics of the building, which SHDs were not jointed to, were confirmed by the forced vibration test. Although this building is linear in a large earthquake, the non-linear member strongly influences the building's vibration characteristics under the small deformation in this test. Furthermore, the performance of the semi-active damper system was identified by a response control test in steady-state vibration. The control law based on LQR for large earthquakes was used.

2. OUTLINE OF BUILDING AND SEMI-ACTIVE DAMPER SYSTEM

2.1. Building with semi-active damper system

The office building in which the semi-active damper system is installed is a five-storey steel structure with PC curtain walls and a basement, and it is located in Shizuoka City, Japan. A typical floor plan, a framework elevation and the configuration of the semi-active damper system are shown in Figure 1. The natural periods of the first three modes of the designed building model in the short side direction are 0.992, 0.352 and 0.222 sec. The system consists of velocity sensors, SHDs, computers and an uninterruptible power supply unit. The velocity sensors are placed on each floor. The eight SHDs are installed between a steel brace and a beam on each storey from the first to the fourth on both gable sides. The computers are established in the control room on the first floor. The elasto-plastic steel dampers are installed in the long-side direction.

2.2. Semi-active hydraulic damper

A full-size SHD that can produce a maximum damping force of 1000 kN with an electric power of only about 70 W has been developed. Its outline is shown in Figure 2(a) and its specifications are shown in Table I. It consists of a cylinder, double rods and a manifold in which several hydraulic units are installed. It is compact and a special establishment place is unnecessary, so a large number of them can be installed in a building. Figure 2(b) shows the hydraulic circuit of the SHD. It comprises a flow control valve, a check valve and an accumulator. The SHD controller converts a damping force command u to a control current Cr to minimize the deviation between an actual damping force f_v and the damping force command u from the computer using the

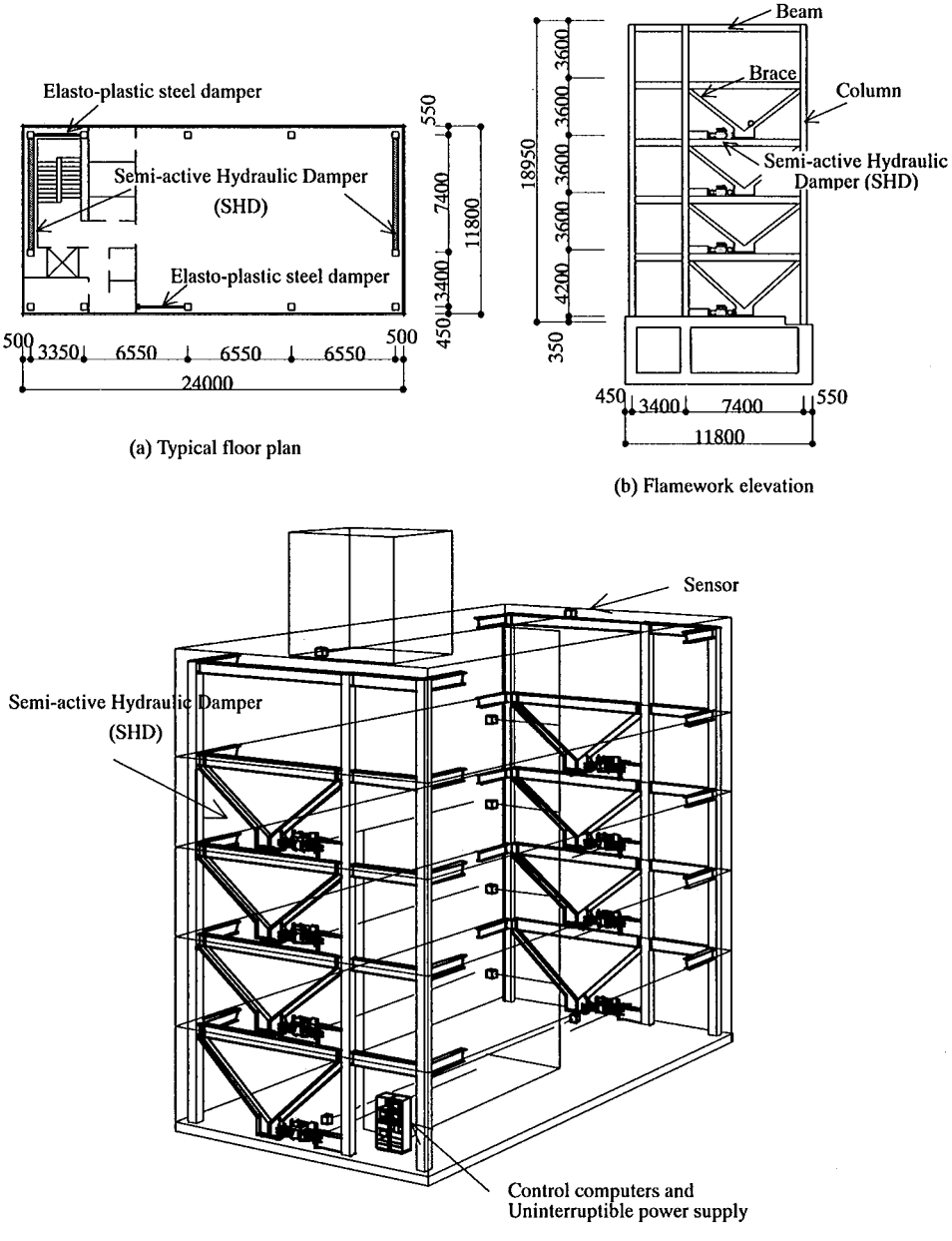

Figure 1. Building outline with SHD: (a) typical floor plan; (b) flamework elevation and (c) configuration of control system.

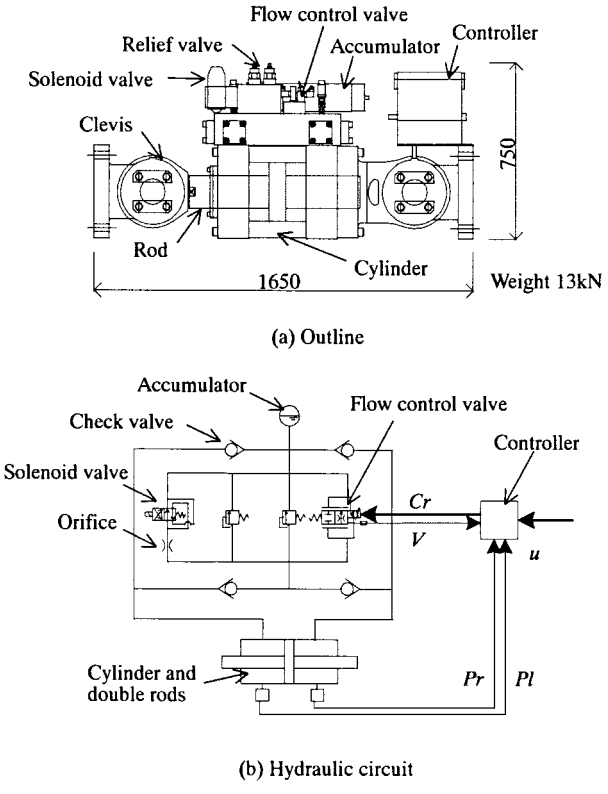

Figure 2. Semi-active hydraulic damper: (a) outline and (b) hydraulic circuit.

Table I. Specification of SHD.

Maximum damping force	1000 kN
Relief load	800–900 kN
Maximum pressure	30 MP
Maximum displacement	$\pm$ 60 mm
Stiffness (including bracket)	$>$ 400 kN/mm
Maximum damping coefficient	$>$ 200 kN sec/mm
Minimum damping coefficient	$<$ 1 kN sec/mm
Maximum velocity	250 mm/sec
Diameter	0.39 m
Weight	13 kN

feedback hydraulic pressure P_1 and P_r, the inside left and right parts of the cylinder, and the actual valve opening V of the flow control valve. If the direction of the damping force command u and the actual damping force f_v are not the same, the sign evaluation circuit introduces an additional valve opening command not to generate the damping force. The controller's parameters are

decided on the basis of the dynamic loading test results to optimize the following performance of the actual damping force to command [9]. A relief valve that opens at a set pressure is installed parallel with the flow control valve, so that the load cannot cause the design stress of the SHD to be exceeded. Furthermore, a solenoid valve that opens in case of an interruption of the electrical service is provided as a fail-safe to an unexpected system fault or power failure. When it opens, the oil flows through the orifice and the SHD works as a passive damper.

2.3. Control system design

The function of the system management, control computation and command transmission are assigned to four computers in the control room on the first floor. It became possible to give the real time control with a 5-ms sampling time and also the system management with high reliability by giving each function to a plural computer. The control procedure was as follows: (i) the sensors measure the building's responses; (ii) the computers calculate the damping force command to minimize the response based on the detected data and (iii) the SHDs generate the damping forces according to the computer's command. By this control procedure, the damping force is optimized and the semi-active control system can obtain the high response reduction performance that is not able to achieve to the passive device.

The sensors measure the absolute acceleration and are able to output the absolute velocity by the analog integration. Also, the relative velocity can be obtained by the calculation in the control computer. The sensors are established permanently and are not for this forced vibration test only. It was recognized that the sensors worked well in actual seismic excitation.

The damping force f_{vi} of the ith SHD can be expressed theoretically with the variable damping element by the following equation:

$$f_{vi} = \begin{cases} f_{\max} \times \operatorname{sign}(v_i), & u_i \times v_i > 0, \quad |u_i| > f_{\max} \\ c_{\max} \times v_i, & u_i \times v_i > 0, \quad \left|\dfrac{u_i}{v_i}\right| > c_{\max}, \quad |u_i| \leqslant f_{\max} \\ c_i(t) \times v_i = u_i, & u_i \times v_i > 0, \quad \left|\dfrac{u_i}{v_i}\right| c_{\max}, \quad |u_i| \leqslant f_{\max} \\ 0, & u_i \times v_i \leqslant 0 \end{cases} \tag{1}$$

where u_i is the damping force command from the computer to the ith SHD and v_i is the i-th SHD's velocity. $f_{\max}$ and $c_{\max}$ are the upper limit values of the damping force and the maximum damping coefficient of the SHD, respectively. They were recognized through the dynamic loading test [9]. The detailed modeling and simulation of the SHD remains as a matter to be discussed further.

The damping force command u_i is the optimal control force, which is designed to minimize the building's response by using the relative velocity feedback law based on a linear quadratic regulator (LQR). The non-linear member does not influence the building's vibration characteristics under the large frame deformation in a large earthquake. Therefore, the problem is treated as a linear problem. This semi-active damper system is designed to control the building's response in linear range during a large earthquake [9]. Although this building is non-linear under the small

deformation in this forced vibration test as shown in Section 4.1, the control law for large earthquakes is used.

The semi-active damping force f_{vi} is non-linear and does not agree with the optimal control force u_i completely. However, the damping force close to optimal control force by LQR is obtained with only a small electrical power. It is easy to obtain the solution of the velocity feedback to the MIMO system by LQR. It is applied most frequently for the semi-active structural control of buildings and civil engineering structures [12–14].

The state equation is

$$\dot{X}(t) = AX(t) + BU(t) + DW(t) \tag{2}$$

where $X = \{x\,\dot{x}\}^{\mathrm{T}}$ is the state vector, U the control force vector and W the disturbance vector. The performance index is

$$J = \int_0^\infty [X(t)^{\mathrm{T}} Q X(t) + U(t)^{\mathrm{T}} R U(t)]\,\mathrm{d}t \tag{3}$$

where Q, and R are the weighting matrices given as

$$Q = \begin{bmatrix} [Q_d] & [0] \\ [0] & [Q_v] \end{bmatrix}, \quad [Q_v] = \mathrm{diag}\,(1), \quad [Q_d] = O, \quad R = \mathrm{diag}\,(r) \tag{4}$$

In this control system design, the problem with the performance index including the control force is treated to study the influence of the maximum damping force to the building's response [9]. The optimal control force without consideration of the disturbance is

$$U(t) = -R^{-1}B^{\mathrm{T}}PX(t) = -GX(t), \quad G = [[G_d]\ [G_v]] \tag{5}$$

where $[G_d]$ and $[G_v]$ are the feedback gain sub-matrix with respect to displacement and velocity, respectively. P is the solution to the following Ricatti equation:

$$PA + A^{\mathrm{T}}P + Q - PBR^{-1}B^{\mathrm{T}}P = 0 \tag{6}$$

The obtained gain is the full matrix with respect to both displacement and velocity. However, since the gain with respect to displacement is negligible, velocity feedback control is adopted, i.e. $[G_d] = O$.

Substituting Equation (5) into Equation (2), the state equation can be expressed as

$$\dot{X}(t) = (A - BG)X(t) + DW(t) \tag{7}$$

Kurata *et al.* [9] calculated the feedback gains for the building model by the changing weighting factor r in Equation (4) and demonstrated the control performance of this system in large earthquakes using the obtained gains. The damping ratio h_i and the natural period T_i of the actively controlled building model to the ith mode obtained by the eigenvalue of $(A - BG)$ in Equation (7) are shown in Figure 3. As r decreases, h_1 and h_2 increase monotonously and T_i is almost constant. Because the SHD is not installed in the fifth storey, the trend of h_3 is different

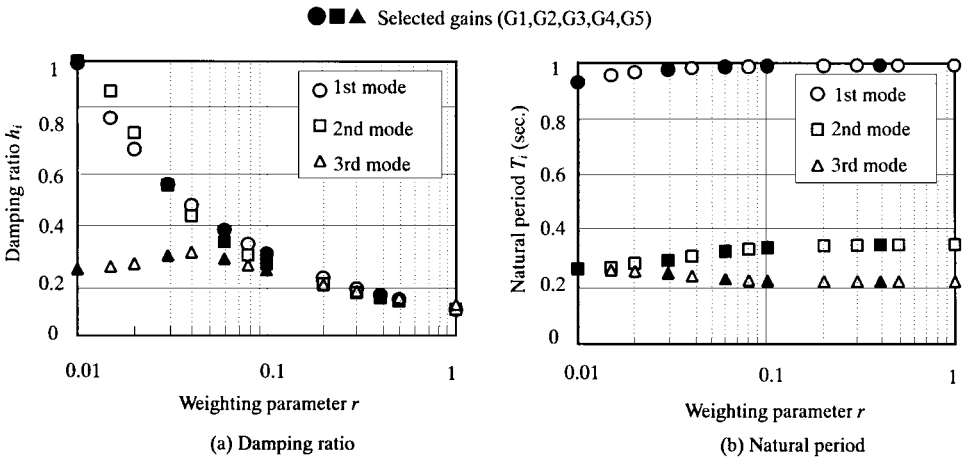

Figure 3. Result of complex eigenvalue analysis of actively controlled building model: (a) damping ratio and (b) natural period.

from those of h_1 and h_2. The typical gain 'G4' for $r = 0.03$, which is chosen on the basis of the simulation analysis results [9], is used for a response control test in steady-state vibration. The first three modes of the actively controlled building model using this gain are at 0.976, 0.297 and 0.251 sec, with associated damping ratios given by 55, 55 and 29 per cent, respectively.

3. TEST METHOD

After completion of the building, a forced vibration test using an exciter was carried out to investigate its vibration characteristics and to determine the system's performance.

3.1. Test environment

A large-scale synchronous exciter with a maximum force of 100 kN, which generates a sinusoidal force by rotating two pairs of eccentric masses, was used. It was placed at the centre of the roof floor of the building and a forced excitation was applied in the short-side direction. The tests were carried out under a constant excitation force. Figure 4 shows the arrangement of exciter and sensors in the building for the test. Displacement sensors were placed on each floor from the basement to the roof at both ends in short-side direction. In addition, sensors for semi-active control were established in each floor as shown in Figure 1(c). For each SHD, the damping force command u, the hydraulic pressures P_l and P_r at the inside left and right parts of the cylinder, and the actual valve opening V of the flow control valve and the control current Cr, shown in Figure 2(b), could be measured by the computer for system management.

3.2. Test cases

Table II shows the test cases. First, the forced vibration test was carried out to confirm the characteristics only of the building to which the SHDs were not joined, corresponding to the

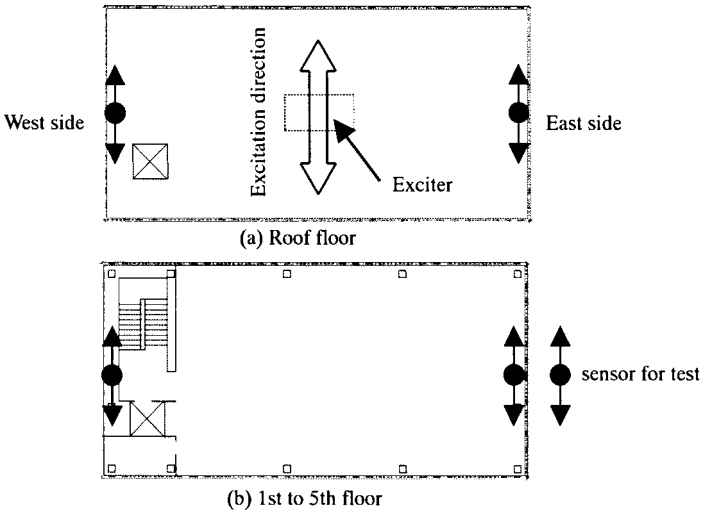

Figure 4. Arrangement of exciter and sensors: (a) roof floor and (b) 1st to 5th floor.

Table II. Test cases.

No.	Cases			Excitation condition	
				Force (kN)	Frequency (Hz)
1	Without SHD			16, 12, 8, 4, 2	0.8–6.0
2	With SHD	Without control	Valve full-open commar	24	0.8–2.0
3			Fail-safe (Passive)	24	0.8–6.0
4		With control	G1, G2, G3, G4, G5*	36	1.2–2.0
5			G4	24	0.8–6.0
6			G4	16	0.8–6.0

* Selected gains shown in Figure 3.

amplitude of the exciting force (without SHD, No. 1). The contribution to the building's stiffness of the secondary members (mainly PC curtain walls) was anticipated to vary according to the amplitude of the excitation force. Hence, tests with different amplitudes were also conducted. Next, after the eight SHDs were joined to the building, a response control test in steady-state vibration was conducted to identify the system's performance (with control, Nos. 4–6). Furthermore, the forced vibration tests for the valve full-open command input preferably avoided producing a damping force, and for the fail-safe as the passive system were carried out (without control, Nos. 2 and 3). The measured frequency ranged from 0.8 or 1.2 to 2.0 Hz for confirmation of the first mode of the building, and from 0.8 to 6.0 Hz for confirmation of the first and second modes. Although a large amplitude of exciting force was desirable to confirm the system's performance, damage to the interior materials of the building was apprehended. Therefore, as the

relative displacement at the roof floor became 5 mm or less, the amplitude of the exciting force was decided. Since the maximum storey drift angle becomes about $\frac{1}{3500}$ or less, the interior materials will be not damaged by excitation.

4. TEST RESULTS

4.1. Building vibration characteristics

The forced vibration test with a constant harmonic excitation force of 16 kN was carried out before the SHDs were jointed to the building (Table II, No. 1). This excitation force amplitude is the upper limit as the relative displacement at the roof floor becomes 5 mm or less and the interior materials will not be influenced by excitation. The resulting resonance and phase lag curves at the east side of the building on the roof, fourth and second floors are shown in Figure 5(a). The vertical axes of the resonance and phase lag curves are the displacement amplitude that scaled the exciting force to 1 kN and the phase delay of the displacement to the exciting force. It can be seen that the first resonant frequency is 1.33 Hz. The resonant amplitude of the second mode at a frequency of 4.7 Hz was small and is omitted from the figure.

Figure 5(b) shows the resonance and phase lag curves around the first resonance frequencies under different excitation forces of 16, 12, 8, 4 and 2 kN. Table III shows the

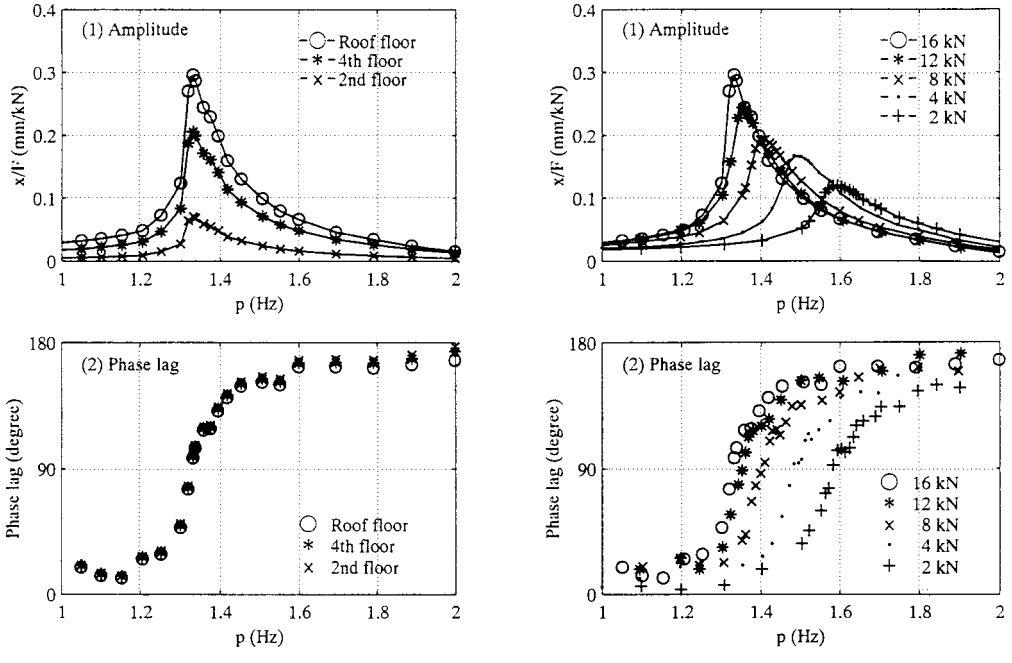

(a) Excitation force of 16 kN

(b) Excitation forces of 16, 12, 8, 4 and 2 kN

Figure 5. Resonance curve for building without SHD: (a) excitation force of 16 kN, (b) excitation forces of 16, 12, 8, 4 and 2 kN.

Table III. Test and analytical results for without SHD.

Test case 1	Test results		Analytical results of SDOF bilinear hysteretic system								
Excitation force (kN)	Resonance frequency (Hz)	Damping ratio (by half-power method)	f_0 (Hz)	h	μ	F/Q_Y	γ	f_e (Hz)	h_{er}	h_{e1r}	h_{e2r}
16	1.33	0.033	1.46	0.013	5.90	0.32	0.82	1.33	0.033	0.019	0.014
12	1.35	0.038	1.46	0.015	4.20	0.28	0.83	1.35	0.038	0.023	0.016
8	1.41	0.045	1.52	0.020	4.10	0.31	0.83	1.41	0.045	0.023	0.022
4	1.48	0.049	1.62	0.022	4.45	0.35	0.83	1.49	0.046	0.022	0.024
2	1.59	0.053	1.72	0.028	3.45	0.34	0.82	1.59	0.057	0.027	0.030

resonance frequency and the damping ratio obtained by the half-power method, together with the analytical results. This will be explained in Section 4.2. They are changed by varying the contribution of the non-structural members to the building's stiffness according to the amplitude of the excitation force. It is considered that a PC curtain wall mainly influences the vibration characteristic of the building. It is connected to the outside of the building with bolts through the sliding element with a certain friction coefficient. The torque for tightening the bolt is designed, as the wall sways freely without the force on the sliding element and does not influence the building's response in a large earthquake. However, as shown in Figure 5(b), the wall strongly influences the building's vibration characteristic under the small deformation in this test. The sliding element of the wall slips along with the increase in exciting force. Therefore, the stiffness of the whole building becomes small and the resonance frequency becomes low. Simultaneously, the influence of friction becomes small and the damping ratio becomes small.

4.2. Approximation of resonance curves by SDOF bilinear hysteretic system

An approximation of resonance curves by the SDOF bilinear hysteretic system is introduced to express the non-linearity of the building without SHDs shown in Section 4.1. The equation of motion for the SDOF system subjected to sinusoidal excitation of magnitude F and frequency p is

$$m\ddot{x} + c\dot{x} + Q(x) = F\cos pt \tag{8}$$

where, m is the mass, c the damping coefficient, $Q(x)$ the non-linear restoring force and x the displacement of the mass.

Rewriting Equation (8) using the equivalent circular frequency $\omega_e(=2\pi\cdot f_e)$ and damping ratio h_e:

$$\ddot{x} + 2\cdot h_e\cdot\omega_e\cdot\dot{x} + \omega_e^2 x = \frac{F}{m}\cos pt \tag{9}$$

The steady-state response of the SDOF system having the bilinear hysteretic restoring force shown in Figure 6 by the equivalent linearization technique [10, 11] is

$$\left(\frac{p}{\omega_0}\right)^2 = C_1(\mu) \pm \sqrt{\frac{f^2}{\mu^2} - \left\{ - S_1(\mu) + 2h\left(\frac{p}{\omega_0}\right)\right\}^2} \tag{10}$$

where $\omega_0 (= 2\pi \cdot f_0)$ is the initial circular frequency and h the initial damping ratio,

$$C_1(\mu) = \begin{cases} \dfrac{1}{\pi}\left[(1-\gamma)\theta^* + \gamma\pi - \dfrac{1-\gamma}{2}\sin 2\theta^*\right], & \delta > \delta_Y \\ 1, & \delta \leqslant \delta_Y \end{cases}$$

$$S_1(\mu) = \begin{cases} -\dfrac{1-\gamma}{\pi}\sin^2\theta^*, & \delta > \delta_Y \\ 0, & \delta \leqslant \delta_Y \end{cases} \tag{11}$$

$$\cos\theta^* = 1 - \frac{2}{\mu}, \quad \mu = \frac{\delta}{\delta_Y}, \quad f = \frac{F}{Q_Y}$$

The equivalent damping ratio in the resonant state ($p = \omega_e$) is

$$h_{er} = h_{e1r} + h_{e2r}, \quad h_{e1r} = -\frac{S_1}{2C_1}, \quad h_{e2r} = \frac{h}{\sqrt{C_1}} \tag{12}$$

Figure 7 compares the test results (Table II, No. 1) of the roof floor displacement with the analytical results of the steady-state response of the SDOF system for an excitation force of 16 kN. The analytical results in Figures 7(a) and 7(b) are by the linear system and by the bilinear hysteretic system (10) with the parameters in Table III. The analytical results by the bilinear

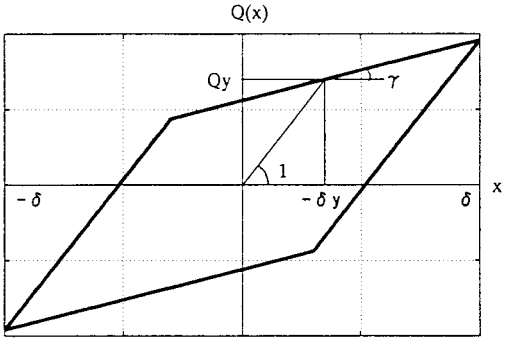

Figure 6. Bilinear hysteretic model.

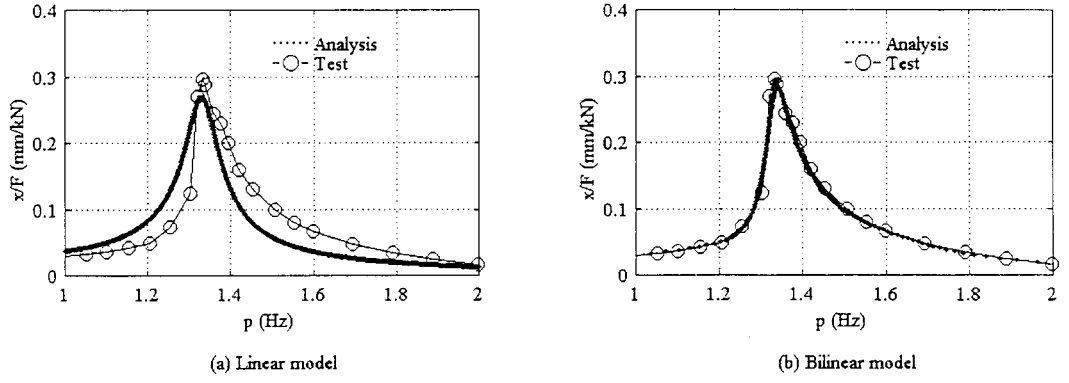

Figure 7. Comparison of test and analytical results (roof floor displacement in case of excitation force of 16 kN): (a) linear model and (b) bilinear model.

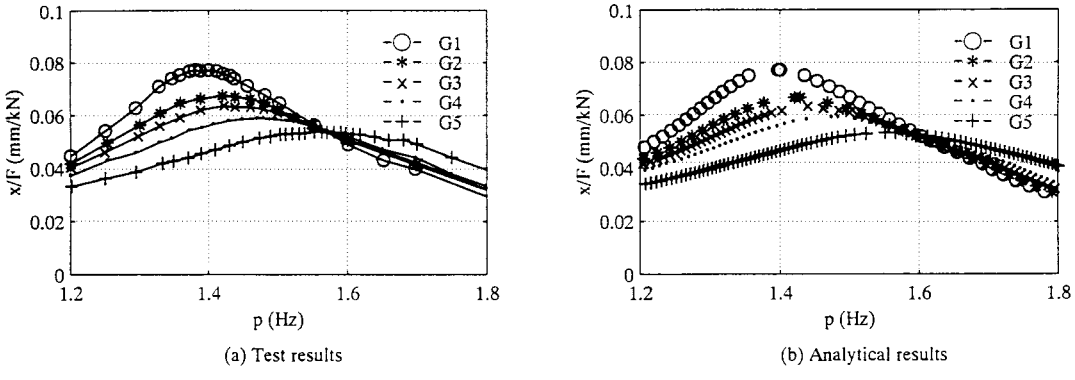

Figure 8. Comparison of test and analytical results (Roof floor displacement in case 4 of excitation force of 36 kN): (a) test results and (b) analytical results.

hysteretic system agree well with the test results. The equivalent natural frequency f_e and damping ratio h_{er} in Table III agree with the test results.

4.3. Performance verification of semi-active damper system

After the eight SHDs were jointed to the building, the response control test in the steady-state vibration was conducted to verify the system's performance. Since a large amplitude level of exciting force was desirable, a constant harmonic excitation force of 36 kN was applied to the building for the control cases of five gains (Table II, No. 4). The resulting resonance curves for the roof floor displacement around the first resonance frequency are shown in Figure 8(a). It can be seen that the first resonance frequency becomes high and the amplitude becomes small along with the increase in gain. Even the non-linearity of the building shown in Section 4.1 influences the change in the resonance frequency. Figure 8(b) shows the analytical results for the

Table IV. Comparison of test and analytical results.

Test cases				Test results	Analytical results of SDOF bilinear hysteretic system								
	Excitation force (kN)		Control condition	Resonance frequency (Hz)	f_0 (Hz)	h	μ	F/Q_Y	γ	f_e (Hz)	h_{er}	h_{e1r}	h_{e2r}
(a)	36	With control	Gain G1	1.38	1.46	0.088	1.85	0.40	0.85	1.40	0.117	0.025	0.091
			Gain G2	1.42	1.48	0.107	1.60	0.40	0.85	1.42	0.134	0.024	0.110
			Gain G3	1.42	1.50	0.115	1.52	0.40	0.85	1.44	0.140	0.023	0.118
			Gain G4	1.47	1.53	0.125	1.42	0.40	0.85	1.47	0.148	0.021	0.127
			Gain G5	1.56	1.57	0.144	1.28	0.40	0.85	1.55	0.163	0.017	0.146
(b)	24	With control	Gain G4	1.57	1.67	0.105	2.80	0.68	0.87	1.57	0.135	0.024	0.111
		Without control	Valve full-open command	1.33	1.54	0.024	7.30	0.59	0.74	1.33	0.053	0.026	0.027
			Fail-safe	1.41	1.54	0.064	4.25	0.69	0.80	1.40	0.097	0.027	0.070
(c)	16	With control	Gain G4	1.62	1.74	0.080	2.35	0.50	0.80	1.59	0.121	0.035	0.085
		Without SHD		1.33	1.46	0.013	5.90	0.32	0.82	1.33	0.033	0.019	0.014

steady-state response of the SDOF bilinear hysteretic system defined by Equation (10) with the parameters in Table IV (a). These results agree well with the test results. The equivalent damping ratio h_{er} is composed of h_{e1r} and h_{e2r}. The parameters h_{e1r} and h_{e2r} are considered to show the damping effect by the non-linear restoring force of the PC curtain wall and by the building's frame itself and SHD control. The latter increases conspicuously along with the increase in gain. Figure 9 shows the time history of the damping force command, the damping force and the valve opening rate for the SHD located on the first and third floors applying an exciting force of 36 kN

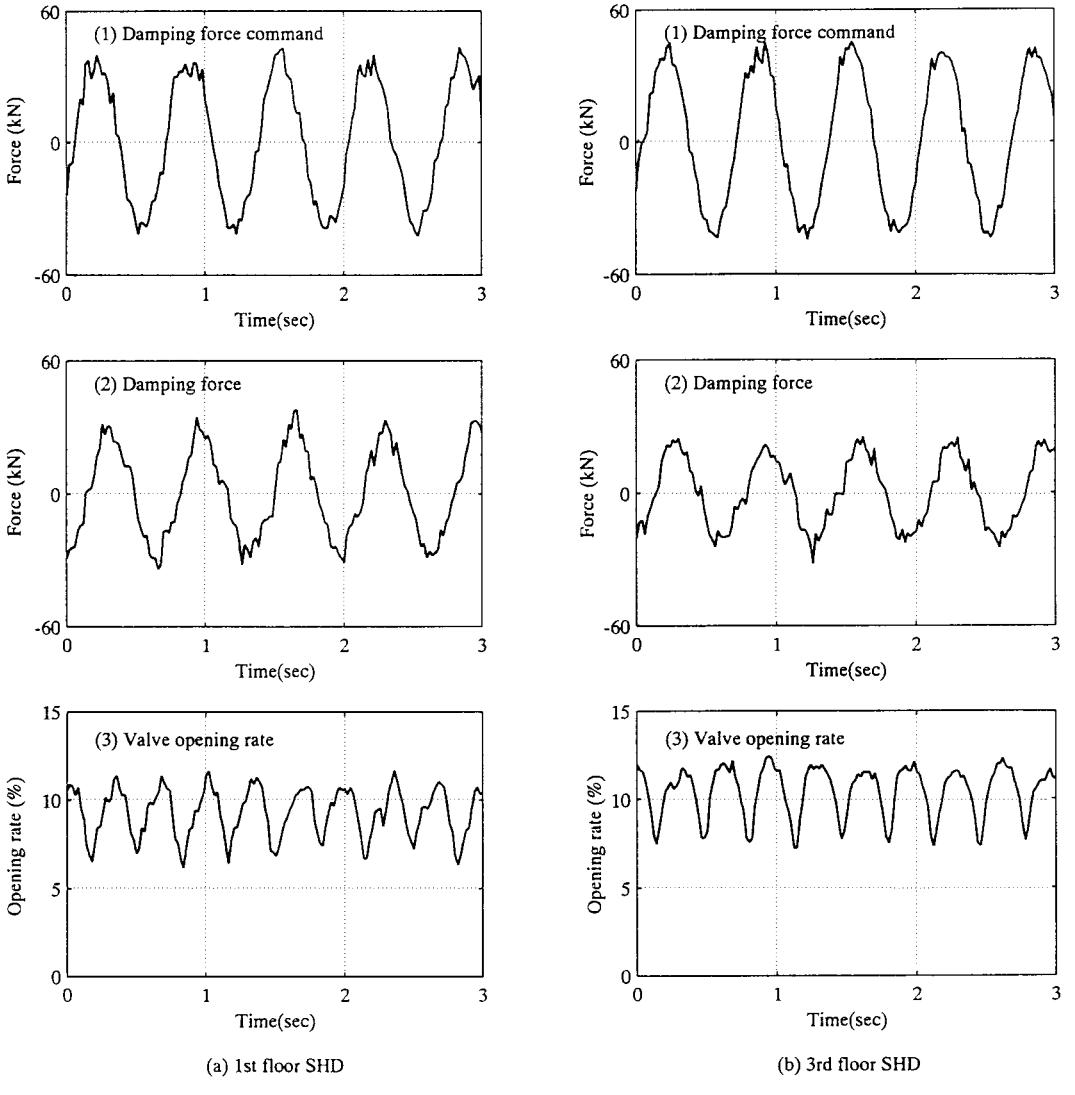

Figure 9. Time history of SHD controlled by gain G4 in case 4 with excitation force of 36 kN and frequency of 1.47 Hz.

at a resonance frequency of 1.47 Hz for the case of gain G4. The damping force command is calculated from the measured velocity of each building floor. The valve opening of the SHD is controlled by the command, and the damping force is generated. It can be seen that the constitution element of the system demonstrates the specified performance. Phase delay occurs between the stroke of the SHD and the storey drift due to the influence of the wall in this amplitude range. The total maximum damping forces of the two SHDs in the first and third storeys are 68.9 and 62.1 kN. However, the storey shear forces in the first and third storeys, calculated by summing the multiplication of mass and measured maximum acceleration on each floor, are 280.9 and 227.2 kN.

A constant harmonic excitation force of 24 kN was applied to the building for the case of SHD control using the gain G4 (Table II, No. 5), where the valve-full-open command was transmitted to all the SHDs (Table II, No. 2), and case of the fail-safe as a passive damper (Table II, No. 3). This excitation force amplitude is the upper limit for the valve-full-open command as the relative displacement at the roof floor becomes 5 mm or less. The resulting resonance curves for the roof floor displacement around the first resonance frequency are shown in Figure 10(a). The peak amplitude for fail-safe and SHD control was reduced to 60 and 40 per cent of that for the valve-full-open command. The parameters shown in Table IV (b) correspond to the analytical results shown in Figure 10(b). The parameter h_{e2r} for the valve-full-open command goes up to 0.027, because pressure loss exists inside the SHD. However, h_{e2r} for SHD control and fail-safe increases to 0.111 and 0.07, respectively.

Finally, for SHD control using the gain G4 and without SHD were compared to confirm the system's control performance for a constant excitation of 16 kN (Table II, Nos. 6 and 1). The resulting resonance curves for the roof floor displacement around the first resonance frequency are shown in Figure 11(a). The peak amplitude with SHD control was reduced to 20 per cent of that without SHD. The parameters shown in Table IV(c) correspond to the analytical results shown in Figure 11(b). The parameter h_{e2r} for SHD control increases to 0.085, compared to 0.014 for without SHD. Incidentally, the parameter h_{e1r} increases from 0.019 to 0.035 along with the decrease in amplitude due to SHD control.

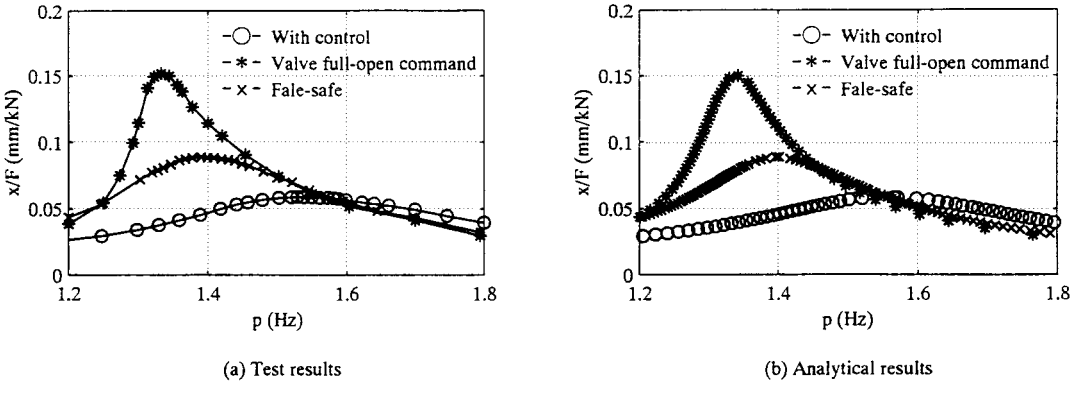

Figure 10. Comparison of test and analytical results (roof floor displacement in case 2, 3 and 5 of excitation force of 24 kN): (a) test results and (b) analytical results.

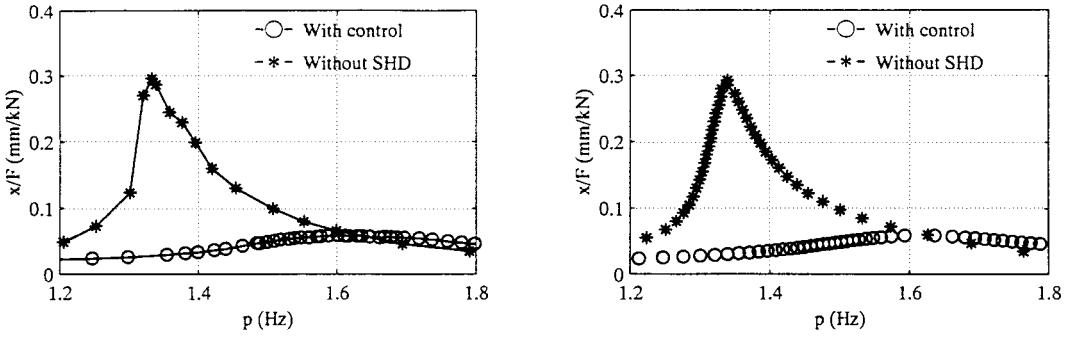

Figure 11. Comparison of test and analytical results (roof floor displacement in case 1 and 6 of excitation force of 16 kN): (a) test results and (b) analytical results.

5. CONCLUSIONS

The authors developed a semi-active hydraulic damper (SHD) and installed it in an actual building in 1998. A forced vibration test with an exciter with a maximum force of 100 kN was carried out to investigate the building's vibration characteristics and to determine the performance of the semi-active damper system. As a result, the primary resonance frequency and the damping ratio of the building to which the SHDs were not jointed, decreased as the exciting force increased with the influence of the non-linear members. The resonance curves of the top displacement of the building can be expressed by the steady-state response of the SDOF bilinear hysteretic system.

After the eight SHDs were jointed to the building, the system's performance was identified by the response control test in steady-state vibration. The damping force command was calculated from the measured velocity of each floor of the building. Then, the valve opening of the SHD was controlled by the command and the damping force was generated. The elements that composed the semi-active damper system demonstrated the specified performance and the whole system operated well. Furthermore, the additional damping effect by the SHD control was evaluated quantitatively through the examination using the SDOF bilinear hysteretic system. The parameter h_{e2r} with SHD control increased to 0.085, compared with 0.014 without SHD for a constant excitation of 16 kN.

ACKNOWLEDGEMENTS

The authors would like to express their gratitude to Mr Y. Matsunaga of Kajima Corporation for developing the SHD, to Mr Y. Higa of Artes Corporation for implementing the forced vibration test and to Kawasaki Heavy Industries Ltd for manufacturing the SHD.

REFERENCES

1. Kobori T. Mission and perspective towards future structural control research. *Proceedings of the 2nd World Conference on Structural Control*, vol. **1**, 1998; 25–34.

2. Housner GW, Bergman LA, Caughey TK, Chassiakos AG, Claus RO, Masri SF, Skelton RE, Soong TT, Spencer Jr. BF, Yao JTP. Special issue: structural control: past, present, and future. *Journal of Engineering Mechanics* ASCE 1997; **123**(9):897–971.
3. Kobori T, Takahashi M, Nasu T, Niwa N, Ogasawara K. Seismic response controlled structure with active variable stiffness system. *Earthquake Engineering and Structural Dynamics* 1993; **22**:925–941.
4. Patten WN. Field test of an intelligent stiffener for bridges at the I-35 Walnut Creek Bridge. *Earthquake Engineering and Structural Dynamics* 1999; **28**:109–126.
5. Kobori T, Takahashi M, Niwa N, Kurata N. Research on active seismic response control system with variable structure characteristics—feedback control with variable stiffness and damping mechanism. *Journal of Structural Engineering*. AIJ 1991; **37**(B):193–202.
6. Kurata N, Kobori T, Takahashi M, Niwa N, Kurino H. Shaking table experiment of active variable damping system. *Proceedings of the 1st World Conference on Structural Control*, vol. **2**, 1994; TP2 108–117.
7. Kurata N, Kobori T, Takahashi M, Niwa N. Study on active variable damping system for high-rise buildings in large earthquakes. *Proceedings of the 1st European Conference on Structural Control*, 1996; 402–409.
8. Kurata N, Kobori T, Takahashi M, Niwa N. Semi-active damper system in large earthquakes. *Proceedings of the 2nd World Conference on Structural Control*, vol. **1**, 1998; 359–366.
9. Kurata N, Kobori T, Takahashi M, Niwa N, Midorikawa H. Actual seismic response controlled building with semi-active damper system. *Earthquake Engineering and Structural Dynamics*, 1999; **28**:1427–1447.
10. Caughey TK. Sinusoidal excitation of a system with bilinear hysteresis. *Journal of Applied Mechanics* 1960; 640–643.
11. Caughey TK. Equivalent linearization techniques. *Journal of Acoustical Society of America* 1963; **35**(11):1706–1711.
12. Symans MD, Constantinou MC. Seismic testing of a building structure with a semi-active fluid damper control system. *Earthquake Engineering and Structural Dynamics* 1997; **26**:759–777.
13. Dowdell DJ, Cherry S. Structural control using semi-active friction dampers. *Proceedings of the 1st World Conference on Structural Control*, vol. **1**. 1994; FA1 59–68.
14. Hirai J, Naruse M, Abiru H. Structural control with variable friction damper for seismic response. *Proceedings of the 11th World Conference on Earthquake Engineering* Paper No. 1934, 1996.

